Cerebral Cortex November 2013;23:2677–2689
doi:10.1093/cercor/bhs256
Advance Access publication August 23, 2012

Is There "One" DLPFC in Cognitive Action Control? Evidence for Heterogeneity From Co-Activation-Based Parcellation

Edna C. Cieslik[1,2,3,4], Karl Zilles[1,2,5,6], Svenja Caspers[1,2], Christian Roski[1,2], Tanja S. Kellermann[1,2,3], Oliver Jakobs[1,3], Robert Langner[1,2,4], Angela R. Laird[7], Peter T. Fox[7] and Simon B. Eickhoff[1,2,4,5]

[1]Institute of Neuroscience and Medicine, INM-1, Research Centre Jülich, Germany, [2]Institute of Neuroscience and Medicine, INM-2, Research Centre Jülich, Germany, [3]Departments of Psychiatry, Psychotherapy, and Psychosomatics, RWTH Aachen University, Aachen, Germany, [4]Institute for Clinical Neuroscience and Medical Psychology, University of Düsseldorf, Germany, [5]JARA-Brain, Translational Brain Medicine, Jülich/Aachen, Germany, [6]C. and O. Vogt Institute for Brain Research, University of Düsseldorf, Düsseldorf, Germany and [7]Research Imaging Institute, University of Texas Health Science Center at San Antonio, San Antonio, TX, USA

Address correspondence to Edna C. Cieslik, Institute for Neuroscience and Medicine (INM-2), Research Center Jülich, D- 52425 Jülich, Germany. Email: e.cieslik@fz-juelich.de

The dorsolateral prefrontal cortex (DLPFC) has consistently been implicated in cognitive control of motor behavior. There is, however, considerable variability in the exact location and extension of these activations across functional magnetic resonance imaging (fMRI) experiments. This poses the question of whether this variability reflects sampling error and spatial uncertainty in fMRI experiments or structural and functional heterogeneity of this region. This study shows that the right DLPFC as observed in 4 different experiments tapping executive action control may be subdivided into 2 distinct subregions-an anterior-ventral and a posterior-dorsal one - based on their whole-brain co-activation patterns across neuroimaging studies. Investigation of task-dependent and task-independent connectivity revealed both clusters to be involved in distinct neural networks. The posterior subregion showed increased connectivity with bilateral intraparietal sulci, whereas the anterior subregion showed increased connectivity with the anterior cingulate cortex. Functional characterization with quantitative forward and reverse inferences revealed the anterior network to be more strongly associated with attention and action inhibition processes, whereas the posterior network was more strongly related to action execution and working memory. The present data provide evidence that cognitive action control in the right DLPFC may rely on differentiable neural networks and cognitive functions.

Keywords: action, connectivity, database, fMRI, prefrontal

Introduction

Flexible, adaptive behavior requires cognitive control, which is the ability to coordinate one's own thoughts and actions in accordance with overarching internally represented goals. Such cognitive control processes become necessary in everyday life when the environmental context changes and automatic or previously learned behaviors are no longer optimal to achieve a goal. A brain region that has consistently been associated with cognitive control processes when complexity or integration demands during action control increases is the dorsolateral prefrontal cortex (DLPFC; Miller and Cohen 2001; Hoshi 2006). Anatomically, the DLPFC encompasses Brodmann's areas (BAs) 9 and 46 (Brodmann 1909), whereas in the macaque monkeys it lies in and around the principal sulcus (Walker's area 46; Walker 1940). The DLPFC is believed to exert its controlling influences through the top-down modulation of task-relevant information processing in, for example, the premotor and posterior parietal associative cortices (MacDonald et al. 2000; Koechlin et al. 2003).

In spite of the well-documented role of the DLPFC in regulating aspects of volitional behavior, studies investigating cognitive control had difficulties in delineating functional divisions within the DLPFC (Duncan and Owen 2000; Wood and Grafman 2003). There is, moreover, considerable variability in the exact location and extension of DLPFC activations across functional neuroimaging experiments investigating cognitive action control. Consequently, it is difficult to compare activations in the DLPFC across different studies and draw conclusions about the specific functional role of the DLPFC in the respective task. One might even ask whether it is possible at all to define the functional role of the DLPFC with classic functional magnetic resonance imaging (fMRI), since this brain region is involved in a variety of cognitive processes (cf. Yarkoni et al. 2011). As it is known that the functional role of a region is partly determined by the neural network it is interacting with, we here used a network-based approach to try to define the specific role of a part of the right DLPFC that showed activation in 4 previous fMRI studies of our group. All 4 studies used different tasks that tapped executive action control and showed activations in the right DLPFC that were located closely together but only overlapped to a moderate degree. The question prompting the current study then was: Does activation of broadly the same region (DLPFC) by different tasks tapping into cognitive action control with moderate overlap between individual effects merely reflect spatial uncertainty of DLPFC activations or may this observation point to an involvement in different neural processes and hence a differentiation within the DLPFC? In this study, we addressed this question by using a DLPFC subregion-defined by 4 previous fMRI studies-as seed for connectivity-based parcellation and hence tested whether distinct subfoci could be identified based on their co-activation patterns across fMRI experiments in the BrainMap database. In a next step, we further investigated differences in functional connectivity between those foci by investigating task-dependent and task-independent connectivity.

A task-dependent approach to investigate connectivity between brain regions has emerged in the last few years with meta-analytic connectivity modeling (MACM) (Laird et al. 2009; Eickhoff et al. 2010; Robinson et al. 2010). MACM relies on defining the brain-wide co-activation patterns of a defined

seed region across a wide number of neuroimaging experiments. MACM may therefore be used to delineate neural networks that are robustly co-activated across many differing experimental tasks (Eickhoff and Grefkes 2011). Moreover, MACM can be used to define the co-activation pattern of each particular seed voxel within a specific volume of interest (VOI). The seed voxels can then be clustered into distinct groups based on similarities and differences in their co-activation profile. MACM can thus be used to generate hypotheses about cortical modules within a chosen VOI and its potential involvement in differential neural networks (Eickhoff, Bzdok et al. 2011).

Moreover, analysis of synchronized spontaneous signal fluctuations (resting-state imaging) has become a widely used tool to investigate functional connectivity between brain regions in the absence of an external task (Beckmann et al. 2005; Damoiseaux et al. 2006; van den Heuvel and Hulshoff Pol 2010). Importantly, it has been shown that these resting-state networks seem to comprise brain regions that are known to share a common behavioral or cognitive function (Biswal et al. 1995; Damoiseaux et al. 2006; van den Heuvel et al. 2009; Laird et al. 2011), prompting the view that resting-state correlations indeed reflect synchronization of intrinsic neuronal activity.

In this context, it should be mentioned that "functional connectivity" has originally been defined in the neuroscience literature as the temporal coincidence of spatially distant neurophysiological events (Aertsen et al. 1989; Friston et al. 1993; Biswal et al. 1995; Lowe et al. 2000). In line with the global definition, MACM allows assessment of task-based functional connectivity (with the unit of observation being the particular neuroimaging experiment), whereas resting-state correlations allow assessment of functional connectivity in an endogenously controlled, task-free state. Given these complementary techniques, a combination of both approaches should yield robust evidence for the "core" of functional connectivity in neural networks.

We used a combination of the 2 methods to define the functional organization as well as its involvement in (potentially distinct) neural networks of the right DLPFC seed region that was defined by merging the DLPFC activation sites from 4 previous studies on action control. The whole-brain co-activation patterns for each voxel within this seed region were computed by an activation likelihood estimation (ALE) meta-analysis of all experiments in the BrainMap database (www.brainmap.org) that reported activation in this location. Clusters within the DLPFC were identified as groups of seed voxels whose whole-brain co-activation profiles were similar to each other and dissimilar to the remaining seed voxels using hierarchical cluster analysis and spectral reordering of cross-correlation matrices. In order to assess whether the delineated clusters show robust differences in their functional connectivity pattern, we performed a conjunction analysis across the (follow-up) MACM analysis of the identified subregions and a resting-state functional connectivity analysis using the same subregions as seeds.

Materials and Methods

Definition of Volume of Interest

We defined a VOI by merging the DLPFC activation sites from 4 previous studies of our group investigating motor control. The first 3 studies (Jakobs et al. 2009; Cieslik et al. 2010; Eickhoff, Pomjanski et al. 2011) used manual stimulus–response tasks requiring a speeded response to a visual stimulus by a button press with either the left or right index finger, whereas the fourth study (Kellermann et al. 2012) used a manual sequence reproduction task:

In the first study (Jakobs et al. 2009), participants were required to respond to centrally presented arrows pointing to one side only (unilateral hand condition) or in a randomized order to either side (random hand condition) by pressing a button with the corresponding index finger. Increased executive control on motor responses was delineated by contrasting random hand with unilateral hand conditions.

The second study employed a manual stimulus–response compatibility task (Cieslik et al. 2010). Here, participants were required to respond to lateralized visual stimuli (dots) with their index finger in a spatially congruent or incongruent manner. Increased executive control was assessed by contrasting incongruent with congruent trials independently of the stimulus or response side.

The third study (Eickhoff, Pomjanski et al. 2011) was a 2-choice reaction-time task similar to the random hand condition of the first study described above. This time, however, the direction of arrows was biased, having a 20%/80% or 80%/20% left/right ratio. Additionally, in some blocks this direction bias was covertly reversed in the middle of the block. Increased executive motor control was delineated by testing for activity parametrically related to the acquisition and adaptation of motor response biases due to changes in the probabilistic structure of the stimuli.

The fourth study was a short-term memory study in which participants had to memorize a visually presented finger-movement sequence consisting of either 4 or 6 items (Kellermann et al. 2012). After a short delay, subjects had to manually reproduce the memorized sequence after a neutral or affective cue. Increased executive control was delineated by comparing activity in the cue period following the memorization of 6-item sequences relative to that following the 4-item sequences.

All 4 studies that differed in the specific demands for executive motor control, showed activation in right DLPFC with partially overlapping but slightly different locations. Following thresholding at $P < 0.05$ (cluster-level family-wise error [FWE]-corrected) of the individual contrasts, the ensuing 4 DLPFC clusters were combined into a single VOI (cluster size: 674 voxels). That is, every single voxel in the VOI region showed activation in at least one of the 4 studies. In a next step, we assessed whether this seed region could be divided into subregions based on similarities and differences between co-activation patterns of the individual seed voxels across neuroimaging experiments.

Meta-Analytic Connectivity Mapping

Co-activation-based parcellation was performed using the BrainMap database (Laird et al. 2009, 2011; www.brainmap.org). From this database, we only included fMRI and Positron emission tomography experiments reporting normal mapping experiments in healthy adults. That is, all experiments involving pathological populations or children were excluded. Likewise, we did not consider any experiments involving, for example, pharmacological interventions or reported group comparisons (e.g. male vs female; left-handed vs right-handed participants). This selection yielded approximately 6200 eligible functional mapping experiments providing coordinates in stereotaxic space, on which all further analyses were based. We here concentrated on experiments reporting activations only and excluded reported deactivations. The rationale behind this approach was that deactivations are reported less consistently in the literature, leading to a rather low amount of available data. Moreover, whereas co-activations between regions may conceptually be interpreted in an unambiguous manner as shared recruitment by task demands, co-deactivations are conceptually more difficult to interpret. The selection of experiments for the MACM analysis and co-activation-based parcellation was only constrained by the requirement to report at least one focus of activation at the respective seed, irrespective of the employed task. There are several reasons for this approach. Apart from undermining the data-driven approach by enforcing a priori constraints, restricting ourselves to a specific behavioral domain (BD) would also entail a conceptual problem. In

particular, it is not well understood how (if) the organization of neural network maps onto the taxonomies that are commonly used to classify mental processes (Poldrack 2006; Laird et al. 2009). In other words, it is well conceivable that different subregions of the region of interest sustain different processes and interact with different networks, although such distinctions may or may not map onto cognitive ontologies. Hence, we tried to derive functional networks in a bottom-up fashion. Therefore, all eligible experiments, that is, all experiments reporting normal functional mapping studies in healthy adults, were included in the MACM analysis.

To enable reliable co-activation mapping for each voxel of the seed region in spite of the variable and usually low number of foci located precisely at a particular voxel, we first identified the set of experiments in BrainMap which reported closest activation. This was achieved by calculating the respective Euclidean distances between the current seed voxel and the individual foci of all experiments. That is, the experiments associated with each seed voxel were defined by activation at or in the immediate vicinity of this particular seed voxel. The brain-wide co-activation pattern for each seed voxel was then computed by quantitative ALE meta-analysis over the hereby associated experiments. To increase reliability, this procedure was repeated then for different degrees of association. In particular, a co-activation map pertaining to any given seed voxel was computed for each set of the closest 30 up to the closest 200 associated experiments in steps of 5 (i.e. closest 30, 35, 40, … , 200 experiments). As can be seen in Supplementary Figure S1 spatial topography (across voxels) was homogenous for different numbers of studies included for spatial remapping. Brain-wide connectivity profiles were averaged across these in order to increase robustness against outliers and potentially confounding effects at a given set-size.

The brain-wide co-activation pattern for each individual seed voxel was then computed by a meta-analysis over the experiments that were associated with that particular voxel by the procedure outlined above. That is, experiments were defined by activation at or close to a particular seed voxel, and quantitative meta-analysis over all foci reported in these experiments was performed to assess how likely any other voxel in the brain showed co-activation with that seed voxel. Meta-analysis was performed using the revised version (Eickhoff et al. 2009, 2012) of the ALE approach. The key idea behind ALE is to treat the reported foci not as single points, but as centers for 3D Gaussian probability distributions that reflect the spatial uncertainty associated with neuroimaging results. For each experiment, the probability distributions of all reported foci are then combined into a modeled activation (MA) map (Turkeltaub et al. 2012). The voxel-wise union of MA-values for all experiments associated with a particular seed voxel then yielded an ALE score for each voxel that describes the co-activation probability of that location with the respective seed voxel. Throughout the different analyses, any test for similarity between 2 seed voxels' connectional fingerprints was performed by calculating a voxel-wise correlation between their whole-brain co-activation maps. We did not perform any thresholding on the connectivity maps to retain the complete pattern of co-activation likelihood. As thresholding would have altered the seed voxels' connectional fingerprint, it may have also skewed the measurement of similarity between them.

Functional Parcellation Based on Co-Activation Patterns

The brain-wide co-activation profiles for all seed voxels were combined into a $N_S \times N_B$connectivity matrix, where N_S is the number of seed voxels (674) and N_B the number of target voxels (~260 000 voxels located within the gray matter) at $2 \times 2 \times 2$ mm^3 resolution. Sets of voxels that feature similar brain-wide co-activation profiles were identified by hierarchical cluster analysis (Timm 2002; Eickhoff et al. 2007). Each voxel initially formed an individual cluster, and a hierarchy was built by progressively merging the least dissimilar cluster to derive successively larger modules. Correlation between the brain-wide co-activation profiles of seed voxels was used as a similarity measure and average linkage criterion for cluster merging (Timm 2002). In sum, the seed voxels were thus merged as a function of correspondence of their co-activation profiles to subdivide the VOI into clusters of convergent functional connectivity.

We, furthermore, also assessed seed voxel clustering using the spectral reordering approach (Johansen-Berg et al. 2004) which involved computing the cross-correlation matrix of the whole brain co-activation profiles obtained for the individual seed voxels and reordering the matrix to minimize the cross-correlation values off the diagonal. Clusters were then identified in the reordered matrix as sets of seed voxels showing strongly correlated connectivity patterns with each other and weakly connectivity patterns with the rest of the matrix (cf. Johansen-Berg et al. 2004; Kim et al. 2010; Eickhoff, Bzdok et al. 2011).

Task-Based Functional Connectivity: Meta-Analytic Connectivity Modeling Analysis

Following the co-activation-based parcellation of the seed regions into subregions, MACM analysis was performed on each of the ensuing clusters in order to characterize their co-activation profiles. In this context, "clusters" refer to sets of voxels within the seed region that were identified by the co-activation-based parcellation outlined above as having similar co-activation patterns to each other but distinct ones to the rest of the seed voxels. The co-activation profiles of the different clusters were obtained by first identifying all experiments in the BrainMap database that featured at least one focus of activation in a particular cluster derived from the co-activation-based hierarchical cluster analysis. In the MACM analysis of the anterior cluster, 283 experiments (from 220 published studies) were included, with a total of 3124 participants. In the MACM analysis for the posterior cluster, 447 experiments (from 316 published studies) were included, with a total of 4279 participants. Details of the experiments in the BrainMap database showing activity in the anterior (Supplementary Table 1) and posterior cluster (Supplementary Table 2) can be found in the Supplementary material.

Next, an ALE meta-analysis was performed on these experiments as described above. In contrast to the MACM underlying the co-activation-based parcellation, where ALE maps were not thresholded to retain the complete pattern of co-activation likelihoods, statistical inference was now performed. To establish which regions were significantly co-activated with a given cluster, ALE scores for the MACM analysis of this cluster were compared with a null-distribution reflecting a random spatial association between experiments with a fixed within-experiment distribution of foci (Eickhoff et al. 2009, 2012). This random-effects inference assesses above-chance convergence between experiments, not clustering of foci within a particular experiment. The observed ALE scores from the actual meta-analysis of experiments activating within a particular cluster were then tested against the ALE scores obtained under this null-distribution yielding a *P*-value based on the proportion of equal or higher random values. The resulting non-parametric *P*-values were transformed into *Z*-scores and thresholded at an FWE-corrected threshold of $P < 0.05$.

Differences in co-activation patterns between the respective clusters were tested by performing MACM separately on the experiments associated with either cluster and computing the voxel-wise difference between the ensuing ALE maps. All experiments contributing to either analysis were then pooled and randomly divided into 2 groups of the same size as the 2 original sets of experiments defined by activation in the first or second cluster (Eickhoff, Bzdok et al. 2011). ALE-scores for these 2 randomly assembled groups were calculated and the difference between these ALE-scores was recorded for each voxel in the brain. Repeating this process 10 000 times then yielded a null-distribution of differences in ALE scores between the MACM analyses of the 2 clusters. The 'true' difference in ALE scores was then tested against this null-distribution yielding a *P*-value for the difference at each voxel based on the proportion of equal or higher random differences. The resulting non-parametric *P*-values were transformed into *Z*-scores, thresholded at $P < 0.001$ and inclusively masked by the respective main effects, that is, the significant effects in the MACM for the particular cluster.

Task-Independent Functional Connectivity: Resting-State Correlations

Resting-state fMRI images were acquired in 100 healthy volunteers (mean age = 45.2, standard deviation [SD] = 14.09, range = 22–71 years) without any record of neurological or psychiatric disorders. All

subjects gave written informed consent to the study protocol, which had been approved by the local ethics committee of the University of Bonn. Before the imaging session, subjects were instructed to keep their eyes closed and just let their mind wander without thinking of anything in particular but not to fall asleep (which was confirmed in post-scan debriefing). For each subject 300 resting-state Echoplanar imaging (EPI) images were acquired using blood-oxygen-level-dependent (BOLD) contrast [gradient-echo EPI pulse sequence, repetition time = 2.2 s, echo time (TE) = 30 ms, flip angle = 90°, in-plane resolution = 3.1 × 3.1 mm, 36 axial slices (3.1 mm thickness) covering the entire brain]. The first 4 scans served as dummy images allowing for magnetic field saturation and were discarded prior to further processing using SPM8 (www.fil.ion.ucl.ac.uk/spm). The EPI images were first corrected for head movement by affine registration using a 2-pass procedure. The mean EPI image for each subject was then spatially normalized to the Montreal Neurological Institute (MNI) single-subject template (Holmes et al. 1998) using the 'unified segmentation' approach (Ashburner and Friston 2005), and the ensuing deformation was applied to the individual EPI volumes. Finally, images were smoothed by a 5-mm full width at half maximum Gaussian to improve signal-to-noise ratio and compensate for residual anatomical variations. The time-series data of each voxel was processed as follows: In order to reduce spurious correlations, variance that could be explained by the following nuisance variables was removed: i) the 6 motion parameters derived from the image realignment; ii) their first derivatives; iii) mean gray-matter, white-matter, and cerebrospinal fluid signal per time point as obtained by averaging across voxels attributed to the respective tissue class in the SPM 8 segmentation; and iv) coherent signal changes across the whole brain as reflected by the first 5 components of a principal component analysis (PCA) decomposition of the whole-brain time series (CompCor approach, cf. Behzadi et al. 2007). All these nuisance variables entered the model as first-order terms and all but the PCA components also as second-order terms as previously described by Behzadi et al. (2007). This procedure was recently shown to increase specificity and sensitivity of the analysis (Chai et al. 2012). Data were then band-pass filtered preserving frequencies between 0.01 and 0.08 Hz, since meaningful resting-state correlations will predominantly be found in these frequencies given that the BOLD response acts as a low-pass filter (Biswal et al. 1995; Greicius et al. 2003; Fox and Raichle 2007). As for the MACM analysis, seed regions of interest were provided by the clusters obtained from the co-activation-based parcellation analysis. Time courses were extracted for all gray-matter voxels within a given cluster. The time course of the seed region was then expressed as the first eigenvariate of these voxels. Linear (Pearson) correlation coefficients between the time series of the seed regions and those of all other gray-matter voxels in the brain were computed to quantify resting-state functional connectivity. These voxel-wise correlation coefficients were then transformed into Fisher's Z-scores and then fed into a second-level analysis of variance (ANOVA) including an appropriate non-sphericity correction as implemented in SPM8. Results were then thresholded to correct for multiple comparisons at a cluster-level FWE rate of $P < 0.05$ (cluster-forming threshold: $P < 0.001$ at voxel level).

Conjunction Between Meta-Analytic Connectivity Modeling and Resting State

The main goal of the connectivity analyses was to determine brain regions that form neural networks for the anterior and posterior DLPFC cluster, respectively. In particular, we aimed at delineating regions that showed significantly stronger task-dependent and task-independent connectivity with the anterior versus posterior cluster and vice versa. We therefore performed a conjunction analysis across the results of MACM and resting-state analysis, restricting assessment of resting-state connectivity differences between the clusters to those voxels showing a significant difference in the co-activation maps from the MACM analysis.

Functional Characterization of the Derived Clusters

Functional properties of the networks ensuing from our co-activation-based parcellation and subsequent connectivity analysis were characterized using the "BD" and "paradigm class (PC)" meta-data categories in the BrainMap database. BDs include the main categories *cognition*, *action*, *perception*, *emotion*, *interoception* as well as their related subcategories, whereas the respective PCs classify the specific task employed (Fox et al. 2005; Turner and Laird 2011). To characterize the functional differences between the studies activating the 2 clusters, we performed quantitative "forward inference" and "reverse inference" (cf. Poldrack 2006; Poldrack 2011) on the 2 networks (right anterior DLPFC-[anterior cingulate cortex] ACC and right posterior DLPFC-posterior parietal cortex). Forward and reverse inferences has become an increasingly used tool to decode mental states from brain imaging activations (cf. Poldrack 2011; Yarkoni et al. 2011; Chang et al. 2012). Whereas "forward inference" is the probability of observing activity in a brain region given the knowledge of the psychological process, "reverse inference" reflects the probability of a psychological process being present given knowledge of activation in a particular brain region (cf. Poldrack 2006). In these analyses, we restricted ourselves to studies dealing with "action" or "cognition" activating either of the 2 ensuing networks. Hence, the performed functional inference is directly contrasting in the networks identified in the present study. In particular, forward inference denotes the probability of activating the anterior (vs posterior) cluster given the respective BD or PC. That is, what is the likelihood that any given experiment from that BD/PC would activate the "right anterior DLPFC-ACC" rather than the posterior "right posterior DLPFC-posterior parietal cortex" network? In contrast, reverse inference describes the probability for any particular BD (or PC) given activation in the anterior or posterior network. That is, given that we see activation of the "right anterior DLPFC-ACC" rather than the "right posterior DLPFC-posterior parietal cortex" network, how likely is a particular BD/PC present. Base rates for activations in the respective network as well as base rates for tasks were taken into account in the latter inference using the Bayesian formulation for deriving P(Task|Activation) based on P(Activation|Task) as well as P(Task) and P(Activation).

Results

Cortical Parcellation Based on Co-Activation Patterns

The co-activation maps for each voxel of the DLPFC seed region were computed by an ALE meta-analysis of those experiments in the BrainMap database that featured the closest activation foci to a given seed voxel. In a next step, ALE values at all voxels in the rest of the brain were combined into a functional co-activation matrix that reflected how likely each seed voxel co-activated with any other voxel in the brain (cf. Eickhoff, Bzdok et al. 2011).

Hierarchical cluster analysis performed on this matrix revealed a separation of the DLPFC seed voxels into 2 co-activation-based clusters: A more anterior-ventral (center of gravity MNI coordinates: 30, 43, 23) and a more posterior-dorsal one (center of gravity MNI coordinates: 37, 33, 32) (Fig. 1).

Anatomically, the 2 clusters laid in the inferior frontal sulcus (covering amongst others areas ifs1 and ifs2, Amunts et al. 2010) and extended into the adjacent middle frontal gyrus (Fig. 2).

At the next lower level of linkage, the more anterior cluster was further subdivided into a rostral and a caudal part. Spectral reordering of the cross-correlation matrix of co-activation profiles (see Supplementary Fig. S2) indicated the same parcellation of the seed VOI as hierarchical cluster analysis, namely a distinction between the anterior-ventral and the posterior-dorsal aspect of the DLPFC and a possible further separation of the anterior cluster into 2 sub-clusters.

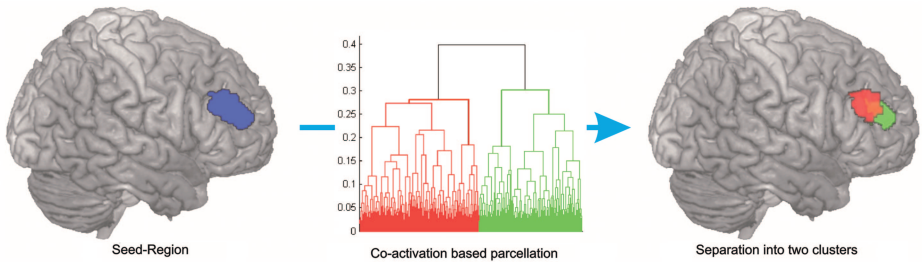

Figure 1. Hierarchical cluster analysis of the co-activation profile matrix revealed a separation of the seed voxels into 2 distinct clusters—an anterior-ventral (in green) and a posterior-dorsal (in red).

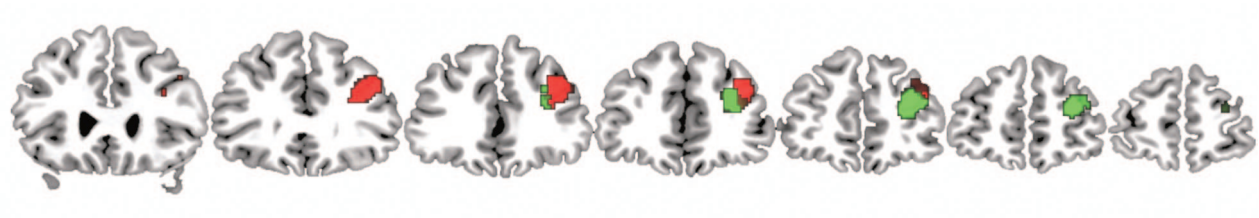

Figure 2. Anatomically, the 2 clusters resulting from the co-activation based parcellation laid in the inferior frontal sulcus extending into the middle frontal gyrus. The more anterior cluster is depicted in green and the more posterior one in red.

However, the consecutively performed analysis of task-dependent and task-independent functional connectivity did not reveal any significant differences corresponding to the separation of the anterior region into 2 subregions. That is, the difference between the clusters formed at the next (second) level of the hierarchical linkage was not strong and/or consistent enough to actually result in discernible network connectivity. The main goal of our co-activation-based parcellation, however, was to test for subregions within the DLPFC seed that are separable on the basis of their functional connectivity profile, reflecting involvement in differentiable networks and functions. Given that only at the level of the 2-cluster solution, the ensuing regions showed significant differences in task-dependent and task-independent functional connectivity, we focused on this parcellation in the results and discussion.

Characterization of Derived Clusters: Task-Dependent and -Independent Connectivity

Task-Dependent Functional Connectivity: Meta-Analytic Connectivity Modeling Analysis

The anterior DLPFC cluster showed significantly stronger task-dependent connectivity than the posterior one with its left homotope (left anterior DLPFC) as well as with the medial superior parietal lobe (SPL; area 7M, Scheperjans, Eickhoff et al. 2008; Scheperjans, Hermann et al. 2008), left area 44 (Amunts et al. 1999), right visual cortex (area hOC3v, Rottschy et al. 2007) and the ACC (see Supplementary Fig. S3*A*). Conversely, the posterior DLPFC cluster showed significantly stronger task-dependent connectivity than the anterior one with its respective left homotope (left posterior DLPFC), bilateral intraparietal sulcus (IPS; areas hIP1, Choi et al. 2006 and hIP3, Scheperjans, Eickhoff et al. 2008; Scheperjans, Hermann et al. 2008), left dorsal premotor cortex (dPMC; area 6, Geyer 2004), left inferior temporal lobe and bilateral anterior–dorsal insula (see Supplementary Fig. S3*B*).

Task-Independent Functional Connectivity: Resting-State Correlations

The anterior DLPFC cluster featured significantly stronger task-independent connectivity than the posterior cluster with its left homotopic region as well as the ACC, the medial SPL (area 5M), left SPL (including areas 7P, 7M), right inferior parietal cortex (areas PGa, PFm; Caspers et al. 2006, 2008), right dPMC (area 6) as well as left ventral insula and bilateral caudate nucleus (see Supplementary Fig. S4*A*). Conversely, the posterior DLPFC cluster showed higher task-independent connectivity than the anterior cluster with a right-hemispheric frontal network including BA 44 as well as rostrally adjacent inferior frontal gyrus and dPMC. Moreover, stronger connectivity was observed with its left homotopic region as well as left inferior frontal gyrus, left area 44, bilateral IPS (hIP1, hIP2, hIP3), bilateral inferior parietal cortex (PFm, PF, PGa), bilateral inferior temporal gyrus, bilateral cerebellum, midcingulate cortex, and pre-supplementary motor area (preSMA) (see Supplementary Fig. S4*B*).

Conjunction Between Meta-Analytic Connectivity Modeling and Resting-State Results

The main goal of this analysis was to identify functional connectivity differences between the anterior and posterior DLPFC clusters that were consistently observed in both types of connectivity analysis. Convergence of both approaches should thus reveal connectivity that is consistently observed across 2 different states of brain function, that is, during the performance of a specific task versus task-free, unconstrained cognition. To this end, we used the cluster-specific co-activation maps from the MACM analysis (as assessed by the contrast analyses detailed in Section 3.2.1) as inference mask for the assessment of the cluster-specific resting-state connectivity (as assessed by the contrast analyses detailed in Section 3.2.2). That is, we assessed the task-based functional connectivity patterns that underlay the observed distinction of our seed into 2 subregions and then tested for common

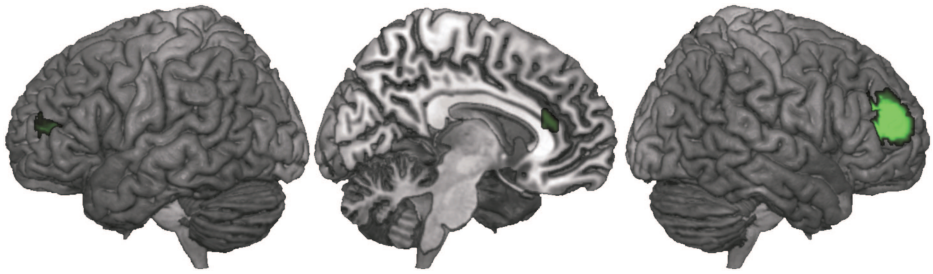

Figure 3. Significantly stronger task-dependent and task-independent connectivity of the anterior versus posterior cluster was observed for its left homotope region and the anterior cingulate cortex.

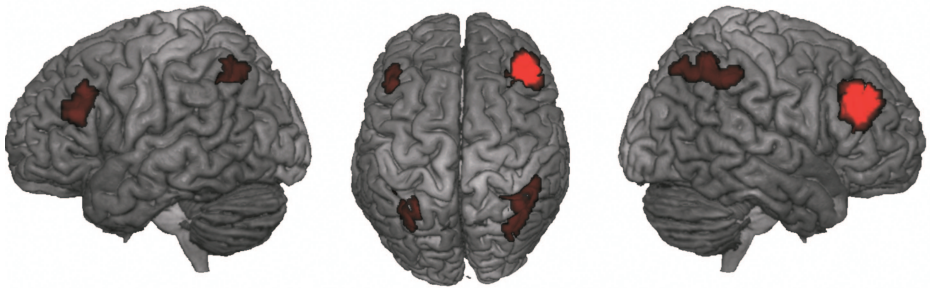

Figure 4. Significantly stronger task-dependent and task-independent connectivity of the posterior versus anterior cluster was observed for its left homotope region and bilateral posterior parietal cortex.

differences in connected networks across 2 complementary methods.

Significantly stronger task-dependent and task-independent connectivity of the anterior versus the posterior cluster was observed for its left homotope region (MNI-coordinates: −30, 53, 12) and the ACC (MNI-coordinates: 9, 33, 18) (Fig. 3).

Conversely, significantly stronger task-dependent and task-independent connectivity of the posterior versus anterior cluster was again found for its left homotope region (MNI-coordinates: −42, 29, 23) as well as for a bilateral region in the IPS (MNI-coordinates: 36, −53, 44/−42, 29, 23; areas hIP1 and hIP3) (Fig. 4).

We furthermore calculated Pearson correlations as a measure of association between the MACM and resting-state connectivity maps of the anterior and posterior clusters, respectively. This revealed correlations of $r = 0.57$ between the 2 connectivity maps for either cluster.

In contrast, maps from opposite networks showed significant anti-correlation. In this analysis, we used the thresholded maps as we specifically wanted to test for the (spatial) correlation of the brain regions significantly connected with either the anterior or posterior cluster. Using the MACM connectivity as the hypothesis-generation dataset and the resting-state for hypothesis-testing, we then showed that those regions where we found significant task-based co-activation for the anterior and posterior networks, respectively, were spatially anti-correlated with the resting-state connectivity pattern of the respective other cluster. That is, the pattern of significant co-activation with the anterior cluster was spatially anti-correlated with the pattern of significant resting-state connectivity with the posterior cluster ($r = -0.30$) and vice versa ($r = -0.45$).

Functional Characterization of Clusters

To characterize the functional differences between the anterior DLPFC-ACC and posterior DLPFC-posterior parietal network in a quantitative manner, we performed forward and reverse inferences (Poldrack 2006; Poldrack 2011) (Fig. 5). Only those BDs and PCs showing significant differences between the 2 networks are depicted. Forward inference describes the probability of observing activity in a brain region given the knowledge of the psychological process, while reverse inference reflects the probability of a psychological process given the knowledge of activation in a specific brain region (cf. Poldrack 2006). The performed forward and reverse inferences revealed that activation in the posterior DLPFC-posterior parietal network (depicted in red) is more related to execution of movement as well as working memory processes such as the *n*-back and Sternberg task. In contrast, the anterior network (depicted in green) is more related to attentional processes and action inhibition as well as tasks requiring conflict resolution like the Go/No-Go and Stroop tasks. That is, reverse inference indeed revealed differences in the functional involvement of the networks characterized by task-dependent and task-independent functional connectivity.

Discussion

We showed that the right DLPFC as observed in 4 different experiments tapping executive action control may be subdivided into 2 distinct subregions based on their whole-brain co-activation patterns across a broad range of neuroimaging studies. Hierarchical cluster analysis revealed a separation of the seed voxels into 2 main clusters: An anterior-ventral and a posterior-dorsal one (Fig. 1). In order to assess whether the 2 delineated clusters show robust differences in their functional connectivity pattern, we performed a conjunction analysis across the (follow-up) MACM analysis of the identified subregions and a resting-state functional connectivity analysis using the same subregions as seeds. This revealed consistent differences in the functional connectivity of the 2 subregions

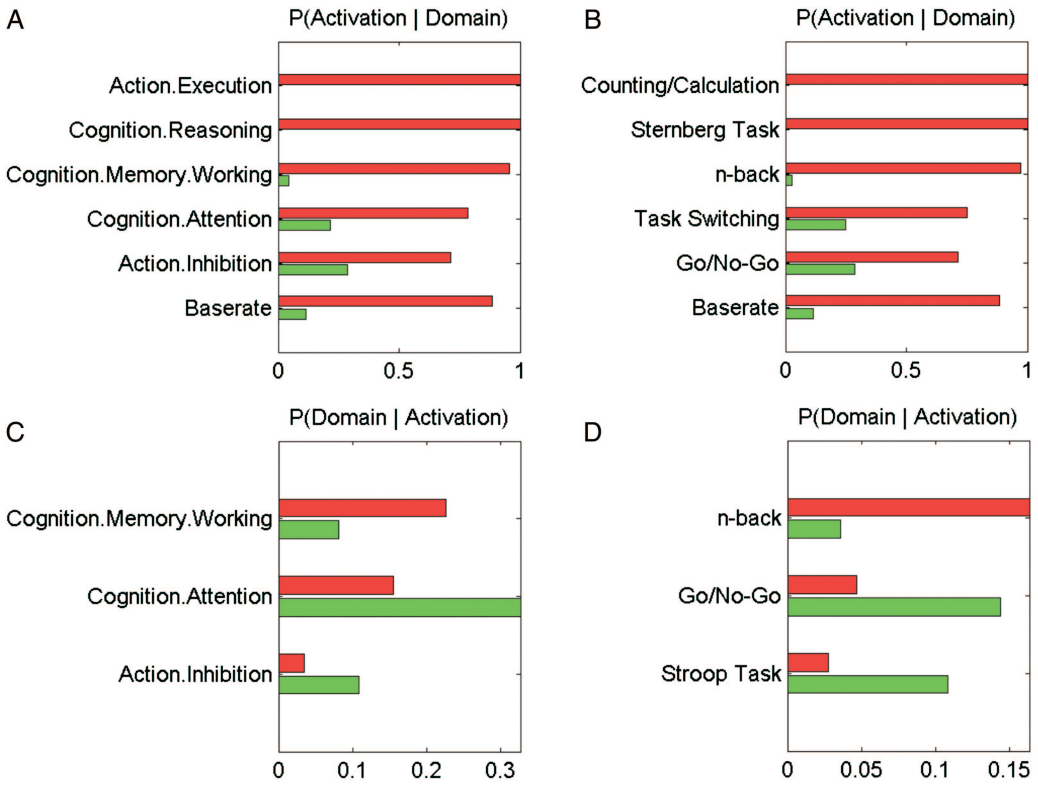

Figure 5. Functional properties were characterized using the "Behavioral Domain" (*A* and *C*) and "Paradigm Class" (*B* and *D*) meta-categories in the BrainMap database. Quantitative forward (*A* and *B*) and reverse (*C* and *D*) inferences revealed functional differences between the anterior (green) and posterior (red) networks.

that are found in both task-dependent and task-independent states. In particular, the anterior cluster showed increased functional connectivity with its left homotopic region and the ACC (Fig. 3), while the posterior cluster showed increased functional connectivity with its left homotopic region and bilateral IPS (Fig. 4). As can be seen in Supplementary Figures S3 and S4, there were also regions showing either only task-dependent or task-independent functional connectivity with the specific cluster. However, as we here focused on networks showing increased functional coupling independently of the current mental state, in the following we will constrain our discussion to the results obtained from the conjunction analysis over MACM and resting state. That is, we will focus on the fundamental distinction between the brain-wide connectivity patterns of the 2 identified clusters, which should be evident in both the task-driven and resting state.

Potential Subregions of the Dorsolateral Prefrontal Cortex and Their Functional Relevance

The DLPFC has been proposed to be involved in the executive "top-down" control of behavior such as when we need to adapt our behavior to a changing environment, override habitual responses or shift between different tasks (Miller and Cohen 2001; Passingham and Sakai 2004; Hoshi 2006; Mansouri et al. 2009). The DLPFC is well positioned to exert control via its rich connections with proximal and distant brain regions. Anatomic connection studies in non-human primates have shown the DLPFC to receive input from distinct regions within the parietal lobes (Petrides and Pandya 1984; Cavada and Goldman-Rakic 1989; Andersen et al. 1990; Petrides and Pandya 1999). Furthermore, the DLPFC is reciprocally interconnected with motor areas in the medial frontal lobe such as the SMA and preSMA, the rostral cingulate cortex, the premotor cortices as well as the cerebellum and the superior colliculus (Goldman and Nauta 1976; Bates and Goldman-Rakic 1993; Lu et al. 1994; Schmahmann and Pandya 1997; Petrides and Pandya 1999). Moreover, the DLPFC is well interconnected with other parts of the prefrontal cortex (PFC; Barbas and Pandya 1989; Miller and Cohen 2001) and is able to represent many types of information, reaching from object and spatial information to response and reward outcomes as well as action strategies (Hoshi 2006). Therefore, the DLPFC is considered as a key area for the integration of sensory information with behavioral intentions, rules and rewards. This information integration is thought to result in the facilitation of the currently most relevant action by exerting cognitive control over motor behavior.

Even though the involvement of the DLPFC in behavioral control is well established, the exact location and extent of activation sites vary across fMRI studies (e.g. Cole and Schneider 2007; Nee et al. 2007; Vogt et al. 2007; Yamaguchi et al. 2008). This variability raises the question if it reflects functional heterogeneity in this region or simply is a result of small sample sizes and spatial uncertainty in fMRI experiments. We here used a network-based approach to investigate this question. A seed region was defined by merging activations from 4 fMRI studies lying in the right DLPFC. We tested for a possible parcellation of this seed region based on co-activation patterns across studies in the BrainMap database. The results of our study argue for the functional heterogeneity

of this right DLPFC seed region. Moreover, investigating task-dependent as well as task-independent functional brain networks pointed towards differential functional roles of the resulting clusters.

We observed increased connectivity between the posterior (vs anterior) portion of the DLPFC and the posterior parietal cortex. This part of the parietal lobe, especially the IPS, is a multimodal region computing space- and object-related information (see, e.g. Corbetta and Shulman 2002; Grefkes and Fink 2005; Caspers et al. 2011). Moreover, activity in IPS is modulated by various behavioral factors such as expected reward, behavioral context, and goals, as well as memory for past events (Thompson and Bichot 2005; Gottlieb 2007). As the IPS shows anatomical connections with the DLPFC (Petrides and Pandya 1984), the IPS has been proposed to act as a salience-specific behavioral integrator, binding visual-spatial, motor, and memory information under the influence of DLPFC top-down control (Gottlieb 2007). We here now showed that especially a posterior portion of the DLPFC shows increased functional connectivity with the parietal cortex, thereby most possibly reflecting a network for cognitive control related to stimulus processing and the selection of relevant information for behavior.

In contrast, for the anterior (vs posterior) DLPFC cluster, increased functional connectivity was found with the ACC. This resonates well with the results from a diverse range of fMRI studies investigating cognitive control, which indicate that the DLPFC and the ACC (BAs 24 and 32) are specifically activated when the demands for cognitive control and monitoring increase due to conflict in information processing and competing response plans (Duncan and Owen 2000; Gehring and Knight 2000; MacDonald et al. 2000; Bunge et al. 2002; Liston et al. 2006; Cole and Schneider 2007; Sohn et al. 2007). According to the error likelihood model (Brown and Braver 2005) ACC activity predicts the probability of making a response error in a given behavioral context. Depending on this probability, the ACC then recruits the DLPFC and both structures may act together, modulating activity in other structures according to the task demands (see also Johnston et al. 2007). Moreover, Dosenbach et al. (2006) analyzed data from 10 different tasks and found the ACC—together with the anterior insula—to show reliable start-cue and sustained activations across the tasks. As these regions furthermore carried error-related signals, they were proposed as a core system for the implementation of task sets related to processes necessary for the selection, implementation, and maintenance of action sets (Dosenbach et al. 2006). According to another hypothesis, the ACC, and anterior insula have been discussed to form a so-called saliency network (SN; cf. Menon and Uddin 2010). Thereafter, the SN shows involvement not only in cognitively demanding tasks such as attentional and response-selection paradigms (Menon et al. 2001; Ridderinkhof et al. 2004) but also responds to uncertainty and emotional salience (Peyron et al. 2000; Grinband et al. 2006). Therefore, it has been proposed that this network is not task-specific but saliency-driven, playing a role in recruiting relevant brain regions for the processing of information.

This study found that the anterior portion of the DLPFC showed increased functional connectivity with the ACC. Hence, it appears that this subregion is especially involved in higher cognitive processes of action control. That is, the anterior portion of the DLPFC identified by co-activation-based parcellation should most likely be involved in a network for higher-level action control in situations in which increased performance monitoring and control adjustments are needed.

It should be kept in mind that the neural networks identified here were based on using only the right DLPFC as a seed region, since all but one seed-defining studies showed activation of exclusively the right DLPFC and not the left. Even though lateralization of the PFC is not well understood yet, there is evidence supporting the notion of a dominance of right DLPFC in monitoring operations (Shallice 2004; Vogt et al. 2007) and resolution of conflict during motor response execution (Aron et al. 2003; Aron et al. 2004; Nee et al. 2007), which may underlie this observation. As supporting evidence for the notion of a right lateralization for cognitive action control in the PFC, we tested for a possible lateralization of studies investigating "action" and "cognition" in the BrainMap database. Therefore, the right DLPFC VOI was flipped to the left side and subsequently tested which studies in the BrainMap database investigating "action" and "cognition" showed activation in the left and right DLPFC seed region respectively. This analysis revealed that when testing for studies investigating "action" or "cognition" 594 studies were found to activate in the right DLPFC seed region but only 177 of that studies also showed activation in the left DLPFC. That is, a right-only activation pattern was seen in 71% of these studies. When looking for studies investigating "action" and "cognition", we found 61 studies activating in the right DLPFC seed region but only 15 of these studies also showed activation in the left DLPFC. The proportion of studies showing activation only on the right side (76%) is very similar to that seen for all studies investigating action or cognition as well as to that seen in our sample of 4 fMRI studies. This analysis hence provides further evidence for a right lateralization in the PFC for cognitive action control. From this starting point, restricting the analysis to the right DLPFC was the most natural choice. In that context, however, it is interesting to note that the 2 identified subregions showed distinct locations of contralateral connectivity, which raises further questions about the relationship of hemispheric specialization and transcallosal connections between left and right DLPFC, which need to be addressed in future studies. A possible interpretation for the finding that both DLPFC-clusters showed increased connectivity with its respective homotope region in the left hemisphere can be found in the literature of task difficulty. Here, fMRI as well as near-infrared spectroscopy studies have shown that simple task usually show more lateralized activation. However, when the complexity of a task increases activation becomes more bilateral (Klingberg et al. 1997; Helton et al. 2010). In line with this Nebel et al. (2005), investigating the neural substrates of focused and divided attention, found that the network components associated with attention processes (in particular, prefrontal and parietal areas) become more bilaterally active depending on task complexity. Under less demanding conditions the authors found mainly right-sided activation. However, when the task difficulty increased, right-sided structures not only increased their activity but were also accompanied by left lateralized homolog areas. We would hence argue that our finding of increased connectivity of the anterior and posterior clusters with their respective left

homotope region reflect an increased interhemispheric information transfer that may be particularly relevant in the context of increased executive demands.

Allocation of Original fMRI-Activations to the Clusters

It is important to note the 4 original fMRI studies were not evenly distributed across the 2 clusters (see Supplementary Fig. S5). The more anterior cluster encompassed almost all of the activation found in the first fMRI study (Jakobs et al. 2009; see Supplementary Fig. S5*A*) and large parts of the activation found in the second study (Cieslik et al. 2010; see Supplementary Fig. S5*B*). In the first study, the DLPFC activation was isolated when contrasting conditions in which the participants did not know the side of the required movement direction compared with conditions in which the participants had to respond to one side only. In the second study, the DLPFC showed increased activations for conditions in which the participants had to respond to a visual stimulus in an incongruent manner compared with conditions in which they had to respond in a congruent manner. Behavioral data showed more errors in the uncertain condition compared with the unilateral hand condition (first study) as well as in the incongruent compared with the congruent condition (second study). Hence, it seems that in both studies the demand of motor control was increased due to competing response plans between the 2 hands. This interpretation would fit well with the observation that the 2 studies majorly overlapped with the anterior cluster that we here have proposed to be part of an anterior-DLPFC-ACC network associated with performance and error monitoring.

The more posterior cluster, in contrast, encompassed most part of the activation found in the third (Eickhoff, Pomjanski et al. 2011; see Supplementary Fig. S5*C*) and fourth (Kellermann et al. 2012; see Supplementary Fig. S5*D*) studies as well as a smaller portion of the activation found in the second study. In particular, the third study laid in the rostral portion of the posterior cluster, whereas the activation found in the fourth study was much broader and encompassed almost all parts of the posterior cluster.

In the third study, activity in the DLPFC was parametrically related to the acquisition and adaptation of motor response biases due to changes in the probabilistic structure of the stimuli. That is, activation in the DLPFC increased when the direction bias of the stimulus was covertly reversed in the middle of the block. In contrast, in the fourth study, the DLPFC showed increased activation when participants had to memorize a 6-item sequence compared with a 4-item sequence, that is, the DLPFC activity was related to an increase in the complexity of finger sequence retrieval. The DLPFC activation in those 2 studies hence seemed to be more related to stimulus processing and acquisition of motor plans involving working memory functions. These results go well along with our finding of the DLPFC activations in these 2 studies to be localized in the posterior cluster that we proposed to build a posterior-DLPFC-posterior parietal network associated with stimulus processing and representation of motor plans.

Quantitative Forward and Reverse Inferences

Forward and reverse inferences revealed that the 2 networks characterized by consistencies across task-dependent as well as task-independent functional connectivity were related to differentiable functional processes. In particular, activation in the anterior network was more related to attentional processes and action inhibition as well as tasks requiring conflict resolution like the Go/No-Go task and the Stroop task. In contrast, the posterior DLPFC-posterior parietal network was more related to the execution of movement as well as working memory processes such as the *n*-back task. These results go well along with the allocation of the 4 original fMRI studies to the 2 clusters. The anterior cluster encompassed primarily the activation in the 2 studies featuring higher demand of action control due to competing response plans between both hands (Cieslik et al. 2010; Jakobs et al. 2009). In these 2 studies subjects showed an increased error rate in the more complex task condition and hence a tendency to respond with the wrong hand. In contrast, the posterior cluster encompassed activation from those 2 studies more related to stimulus processing and acquisition of motor plans involving working memory functions (Eickhoff, Bzdok et al. 2011; Kellermann et al. 2012). In these 2 studies, DLPFC activity was associated with adaptation of motor response biases and with an increase in complexity of motor sequence retrieval.

In summary, quantitative forward and reverse inferences provides further evidence for an involvement of the 2 networks in differentiable functional processes. Whereas the anterior network is more related to attentional processes and processes of action inhibition, the posterior network is more related to action control processes involving working memory functions.

Functional Gradient in Dorsolateral Prefrontal Cortex

Evidence from functional neuroimaging studies has prompted the proposal of models featuring a topographical organization along an anterior-posterior axis in the PFC (e.g. Koechlin et al. 2003; Koechlin and Summerfield 2007; Badre and D'Esposito 2009; Taren et al. 2011). In all of these models, action control is implemented in the PFC along a posterior-to-anterior hierarchy, with progressively anterior regions supporting increasingly abstract representations and complex actions. For instance, the Cascade model of PFC (Koechlin et al. 2003) tries to explain how executive control might be implemented within a hierarchy in the PFC. The model relies on the assumption that competition arises when bottom-up input produces alternative action representations. It furthermore assumes that this competition is resolved in the PFC which maintains overarching contextual information to bias selection of relevant representations over competitors. At the lower level, action selection is based on sensory input and environmental contextual cues, supported by dPMC and posterior DLPFC, respectively. At the higher level, supported by anterior DLPFC, action selection is based on episodic control, taking into account the ongoing temporal context. At the highest level, branching control supported by the frontopolar cortex selects actions based on a pending temporal context. That is, the more posterior parts of the PFC monitors comparatively simple control processes, such as mapping of stimuli to actions, whereas the anterior parts are involved in higher-order processes such as integrating relationships among behavioral rules (cf. Taren et al. 2011). This assumption is well in line with the results obtained from our connectivity analysis showing that subregions of the DLPFC are involved in different functional networks suggesting different

functions in the cognitive control of behavior. While a posterior-DLPFC-posterior-parietal network would accordingly be involved in more basic processes of cognitive control, an anterior-DLPFC-ACC network would be involved in more abstract processes such as the monitoring of performance and adjusting behavior when necessary.

Most studies investigating the topographical organization in the PFC have considered the whole PFC, reaching from the premotor cortices to the frontopolar cortex. The present data demonstrate that even a relatively small region of the DLPFC can be functionally differentiated based on its co-activation pattern (Fig. 1) and that the resulting subdivisions show distinct functional connectivity (Figs. 3 and 4). Moreover, our connectivity analysis mirrors the cascade model predicting a posterior to anterior axis in the PFC with progressively anterior regions involved in increasingly abstract components of action selection (Koechlin et al. 2003).

Analytic Approach and Functional Implication

We used a combination of 2 analytic approaches, that is, analysis of task-dependent as well as task-independent (resting state) connectivity to delineate brain areas functionally coupled with the 2 identified subregions in the DLPFC. MACM allows the delineation of consistently co-activated neural networks across a wide variety of neuroimaging experiments (Eickhoff, Bzdok et al. 2011). Even though MACM does not allow any inference on connectivity in individual participants as the unit of observation is a specific contrast in neuroimaging experiments, it allows us to identify potentially interacting cortical modules based on the co-activation pattern of voxels in a particular seed region. Thereby, MACM can be used to form hypotheses about the differential connectivity between resulting clusters. Task-independent analysis, in contrast, relies on measuring the level of co-activation of spontaneous BOLD signal time series in the absence of an externally structured task (van den Heuvel and Hulshoff Pol 2010). Moreover, analyses of task-independent activity have shown that most resting-state networks represent well-known networks that share common functions (Biswal et al. 1995; Damoiseaux et al. 2006; van den Heuvel et al. 2009). The functional relevance of synchronized neuronal activity has been shown for cognitive processes such as memory formation (Axmacher et al. 2006) as well as selective attention (Womelsdorf and Fries 2007). As neurons show high spontaneous firing activity even in the absence of a specific task, it has been proposed that task-independent connectivity contributes to keeping functional systems in an active state, thereby improving performance and control whenever functional connectivity is needed (cf. van den Heuvel and Hulshoff Pol 2010).

Here, conjunction analysis between task-dependent and task-independent connectivity results revealed 2 networks, an anterior-DLPFC-ACC and a posterior-DLPFC-posterior-parietal network, which showed increased functional coupling independently of the current mental state. That is, the 2 networks are not only differentially co-activated across neuroimaging experiments, as supported by our MACM analysis, but also show differentiated synchronized neuronal coupling in the absence of an externally structured task. As the conjunction analysis highlights regions that have a fundamental functional connectivity with the DLPFC, we would propose that the networks identified here most likely represent networks critical for the functions subserved by the 2 identified DLPFC subregions.

Limitations

It is important to note that the aim of this study was not to define the exact number of subregions within the entire DLPFC. Such an analysis strongly depends on the definition of the brain area used as the region of interest (cf. Mars et al. 2011). As the size of the DLPFC and especially its borders to adjacent brain regions such as the ventrolateral PFC and premotor areas are controversially discussed in the literature (cf. Miller and Cohen 2001; Hoshi 2006; Taren et al. 2011; Tsujimoto et al. 2011) a parcellation of the DLPFC as a whole is challenging. Our aim was thus to investigate, whether the various, partially overlapping fMRI activations we observed in the right posterior DLPFC may point to an underlying differentiation in this region. This specific aim should be highly important from a conceptual point of view, as it demonstrates how co-activation based parcellation may be used to clarify partially overlapping and potentially conflicting findings from previous studies. The aim of this study was thus to show, in a proof-of-principle manner, that closely neighboring and partially overlapping activations in the DLPFC may represent different underlying cortical modules or areas. Importantly, analysis of task-dependent and task-independent functional connectivity analysis also implicated these differentiable networks. Moreover, quantitative reverse inference (Poldrack 2006) provided further evidence for an involvement of these networks in differentiable functional processes (Fig. 5) which should carefully be taken into account when interpreting activations lying in the DLPFC.

However, it has to be noted that we here investigated the functional organization of only a small proportion of the right DLPFC thereby limiting the generalizability of the results towards the DLPFC as a whole. Even though we would assume that the DLPFC as a whole would show an even more diverse differentiation in functional networks, our results relied on the basis of a rather small portion on the DLPFC. Moreover, we used a functional definition of the seed region on the basis of 4 fMRI studies on tapping executive action control. Hence, the subsequent analysis and results strongly depend on the activations found in the previous fMRI studies thereby constraining the robustness of the results to a certain degree.

Conclusion

This study illustrates that closely neighboring activation in behavioral similar task may actually reflect 2 distinct functional modules questioning the common practice of interpreting "near-by" activation in a uniform manner. In particular, we showed that the right DLPFC seed region as obtained from 4 fMRI studies tapping cognitive action control could be subdivided into 2 distinct parts based on their co-activation profile and provided evidence for an anterior-DLPFC-ACC and a posterior-DLPFC-posterior-parietal network. Together with further evidence from quantitative forward and reverse inferences, we propose this region to be organized in a hierarchical fashion. In particular, the more posterior cluster may be involved in action control processes that are more dependent

on the interaction with stimulus processing and working memory. In contrast, the more anterior portion of the DLPFC is most likely involved in higher-order control processes of motor behavior such as the monitoring of motor responses and subsequent behavioral adjustments. In summary, the present data indicate that the executive control of behavior does not engage a single homogenous right DLPFC region but may rely on at least 2 distinct subregions involved in differentiable neural networks and cognitive functions.

Supplementary Material

Supplementary material can be found at: http://www.cercor.oxfordjournals.org/.

Funding

This work was supported by the Human Brain Project (R01-MH074457; to P.T.F., A.R.L. and S.B.E.), the Initiative and Networking Fund of the Helmholtz Association within the Helmholtz Alliance on Systems Biology (Human Brain Model; K.Z., S.B.E.) and the Helmholtz Alliance for Mental Health in an Aging Society (HelMA; K.Z.). Funding to pay the Open Access publication charges for this article was provided by the Central library of the Research Centre Jülich.

Notes

Conflict of Interest: None declared.

References

Aertsen AM, Gerstein G, Habib M, Palm G. 1989. Dynamics of neuronal firing correlation: modulation of "effective connectivity". J Neurophysiol. 61:900–917.

Amunts K, Lenzen M, Friederici AD, Schleicher A, Morosan P, Palomero-Gallagher N, Zilles K. 2010. Broca's region: novel organizational principles and multiple receptor mapping. PLoS Biol. 8 (9):e1000489.

Amunts K, Schleicher A, Bürgel U, Mohlberg H, Uylings HB, Zilles K. 1999. Broca's region revisited: cytoarchitecture and intersubject variability. J Comp Neurol. 412(2):319–341.

Andersen RA, Asanuma C, Essick G, Siegel RM. 1990. Corticocortical connections of anatomically and physiologically defined subdivisions within the inferior parietal lobule. J Comp Neurol. 296:65–113.

Aron AR, Fletcher PC, Bullmore ET, Sahakian BJ, Robbins TW. 2003. Stop-signal inhibition disrupted by damage to right inferior frontal gyrus in humans. Nat Neurosci. 6:115–116.

Aron AR, Robbins TW, Poldrack RA. 2004. Inhibition and the right inferior frontal cortex. Trends Cogn Sci. 8:170–177.

Ashburner J, Friston KJ. 2005. Unified segmentation. NeuroImage. 26:839–851.

Axmacher N, Mormann F, Fernandez G, Elger CE, Fell J. 2006. Memory formation by neuronal synchronization. Brain Res Rev. 52:170–182.

Badre D, D'Esposito M. 2009. Is the rostro-caudal axis of the frontal lobe hierarchical?. Nat Rev Neurosci. 10:659–669.

Barbas H, Pandya DN. 1989. Architecture and intrinsic connections of the prefrontal cortex in the rhesus monkey. J Comp Neurol. 286:353–375.

Bates JF, Goldman-Rakic PS. 1993. Prefrontal connections of medial motor areas in the rhesus monkey. J Comp Neurol. 336:211–228.

Beckmann CF, DeLuca M, Devlin JT, Smith SM. 2005. Investigations into resting-state connectivity using independent component analysis. Phil Trans R Soc Lond B Biol Sci. 360:1001–1013.

Behzadi Y, Restom K, Liau J, Liu TT. 2007. A component based noise correction method (CompCor) for BOLD and perfusion based fMRI. Neuroimage. 37:90–101.

Biswal B, Yetkin FZ, Haughton VM, Hyde JS. 1995. Functional connectivity in the motor cortex of resting human brain using echo-planar MRI. Magn Reson Med. 34:537–541.

Brodmann K. 1909. Vergleichende Lokalisationslehre der Grobhirnrinde. Leipzig: Barth.

Brown JW, Braver TS. 2005. Learned predictions of error likelihood in the anterior cingulate cortex. Science. 307:1118–1121.

Bunge SA, Hazeltine E, Scanlon MD, Rosen AC, Gabrieli JDE. 2002. Dissociable contributions of prefrontal and parietal cortices to response selection. Neuroimage. 17:1562–1571.

Caspers S, Amunts K, Zilles K. 2011. Posterior parietal cortex: Multimodal association cortex. In: Mai JH, Paxinos G, editors. The Human Nervous System, 3rd ed. Amsterdam, (NL): Elsevier. p. 1036–1055.

Caspers S, Eickhoff SB, Geyer S, Scheperjans F, Mohlberg H, Zilles K, Amunts K. 2008. The human inferior parietal lobule in stereotaxic space. Brain Struct Funct. 212:481–495.

Caspers S, Geyer S, Schleicher A, Mohlberg H, Amunts K, Zilles K. 2006. The human inferior parietal cortex: cytoarchitectonic parcellation and interindividual variability. Neuroimage. 33:430–448.

Cavada C, Goldman-Rakic PS. 1989. Posterior parietal cortex in rhesus monkey: II. Evidence for segregated corticocortical networks linking sensory and limbic areas with the frontal lobe. J Comp Neurol. 287:422–445.

Chai XJ, Castañón AN, Öngür D, Whitfield-Gabrieli S. 2012. Anticorrelations in resting state networks without global signal regression. Neuroimage. 59(2):1420–1428.

Chang LJ, Yarkoni T, Khaw MW, Sanfey AG. 2012. Decoding the role of the insula in human cognition: functional parcellation and large-scale reverse inference. Cereb Cortex (in press).

Choi HJ, Zilles K, Mohlberg H, Schleicher A, Fink GR, Armstrong E, Amunts K. 2006. Cytoarchitectonic identification and probabilistic mapping of two distinct areas within the anterior ventral bank of the human intraparietal sulcus. J Comp Neurol. 495:53–69.

Cieslik EC, Zilles K, Kurth F, Eickhoff SB. 2010. Dissociating bottom-up and top-down processes in a manual stimulus–response compatibility task. J Neurophysiol. 104:1472–1483.

Cole MW, Schneider W. 2007. The cognitive control network: integrated cortical regions with dissociable functions. Neuroimage. 37:343–360.

Corbetta M, Shulman GL. 2002. Control of goal-directed and stimulus-driven attention in the brain. Nat Rev Neurosci. 3:201–215.

Damoiseaux JS, Rombouts SA, Barkhof F, Scheltens P, Stam CJ, Smith SM, Beckmann CF. 2006. Consistent resting-state networks across healthy subjects. Proc Natl Acad Sci USA. 103:13848–13853.

Dosenbach NU, Visscher KM, Palmer ED, Miezin FM, Wenger KK, Kang HC, Burgund ED, Grimes AL, Schlaggar BL, Petersen SE. 2006. A core system for the implementation of task sets. Neuron. 50:799–812.

Duncan J, Owen AM. 2000. Common regions of the human frontal lobe recruited by diverse cognitive demands. Trends Neurosci. 23:475–483.

Eickhoff SB, Bzdok D, Laird AR, Kurth F, Fox PT. 2012. Activation likelihood estimation meta-analysis revisited. Neuroimage. 59:2349–2361.

Eickhoff SB, Bzdok D, Laird AR, Roski C, Caspers S, Zilles K, Fox PT. 2011. Co-activation patterns distinguish cortical modules, their connectivity and functional differentiation. Neuroimage. 57: 938–949.

Eickhoff SB, Grefkes C. 2011. Approaches for the integrated analysis of structure, function and connectivity of the human brain. Clin EEG Neurosci. 42:107–121.

Eickhoff SB, Jbabdi S, Caspers S, Laird AR, Fox PT, Zilles K, Behrens TE. 2010. Anatomical and functional connectivity of cytoarchitectonic areas within the human parietal operculum. J Neurosci. 30:6409–6421.

Eickhoff SB, Laird AR, Grefkes C, Wang LE, Zilles K, Fox PT. 2009. Coordinate-based activation likelihood estimation meta-Analysis of

neuroimaging data:a random-effects approach based on empirical estimates of spatial uncertainty. Hum. Brain Mapp. 30:2907–2926.
Eickhoff SB, Pomjanski W, Jakobs O, Zilles K, Langner R. 2011. Neural correlates of developing and adapting behavioral biases in speeded choice reactions—an FMRI study on predictive motor coding. Cereb Cortex. 21:1178–1191.
Eickhoff SB, Rottschy C, Zilles K. 2007. Laminar distribution and co-distribution of neurotransmitter receptors in early human visual cortex. Brain Struct Funct. 212:255–267.
Fox MD, Raichle ME. 2007. Spontaneous fluctuations in brain activity observed with functional magnetic resonance imaging. Nat Rev Neurosci. 9:700–711.
Fox PT, Laird AR, Fox SP, Fox PM, Uecker AM, Crank M, Koenig SF, Lancaster JL. 2005. BrainMap taxonomy of experimental design: description and evaluation. Hum Brain Mapp. 25:185–198.
Friston KJ, Frith CD, Liddle PF, Frackowiak RS. 1993. Functional connectivity: the principal-component analysis of large (PET) data sets. J Cereb Blood Flow Metab. 13:5–14.
Gehring WJ, Knight RT. 2000. Prefrontal–cingulate interactions in action monitoring. Nat Neurosci. 3(5):516–520.
Geyer S. 2004. The mircostructural border between the motor and the cognitive domain in the human cerebral cortex. Advances in Anatomy, Embryology, and Cell Biology. Berlin, Springer.
Goldman PS, Nauta WJ. 1976. Autoradiographic demonstration of a projection from prefrontal association cortex to the superior colliculus in the rhesus monkey. Brain Res. 116:145–149.
Gottlieb J. 2007. From thought to action: the parietal cortex as a bridge between perception, action, and cognition. Neuron. 53:9–16.
Grefkes C, Fink GR. 2005. The functional organization of the intraparietal sulcus in humans and monkeys. J Anat. 207:3–17.
Greicius MD, Krasnow B, Reiss AL, Menon V. 2003. Functional connectivity in the resting brain: a network analysis of the default mode hypothesis. Proc Natl Acad Sci USA. 100(1):253–258.
Grinband J, Hirsch J, Ferrera VP. 2006. A neural representation of categorization uncertainty in the human brain. Neuron. 49:757 –763.
Helton WS, Warm JS, Tripp LD, Matthews G, Parasuraman R, Hancock PA. 2010. Cerebral lateralization of vigilance: a function of task difficulty. Neuropsychologia. 48(6):1683–1688.
Holmes CJ, Hoge R, Collins L, Woods R, Toga AW, Evans AC. 1998. Enhancement of MR images using registration for signal averaging. J. Comput. Assist. Tomogr. 22:324–333.
Hoshi E. 2006. Functional specialization within the dorsolateral prefrontal cortex: a review of anatomical and physiological studies of non-human primates. Neurosci Res. 54:73–84.
Jakobs O, Wang LE, Dafotakis M, Grefkes C, Zilles K, Eickhoff SB. 2009. Effects of timing and movement uncertainty implicate the temporo-parietal junction in the prediction of forthcoming motor actions. Neuroimage. 47:667–677.
Johansen-Berg H, Behrens TE, Robson MD, Drobnjak I, Rushworth MF, Brady JM, Smith SM, Higham DJ, Matthews PM. 2004. Changes in connectivity profiles define functionally distinct regions in human medial frontal cortex. Proc Natl Acad Sci USA. 101:13335–13340.
Johnston K, Levin HM, Koval MJ, Everling S. 2007. Top-down control-signal dynamics in anterior cingulate and prefrontal cortex neurons following task switching. Neuron. 53:453–462.
Kellermann TS, Sternkopf MA, Schneider F, Habel U, Turetsky BI, Zilles K, Eickhoff SB. 2012. Modulating the processing of emotional stimuli by cognitive demand. Soc Cogn Affect Neurosci. 7(3):263–73.
Kim JH, Lee JM, Jo HJ, Kim SH, Lee JH, Kim ST, Seo SW, Cox RW, Na DL, Kim SI et al. 2010. Defining functional SMA and pre-SMA subregions in human MFC using resting state fMRI: functional connectivity-based parcellation method. Neuroimage. 49:2375–2386.
Klingberg T, O'Sullivan BT, Roland PE. 1997. Bilateral activation of fronto-parietal networks by incrementing demand in a working memory task. Cereb Cortex. 7(5):465–471.
Koechlin E, Ody C, Kouneiher F. 2003. The architecture of cognitive control in the human prefrontal cortex. Science. 302:1181–1185.
Koechlin E, Summerfield C. 2007. An information theoretical approach to prefrontal executive function. Trends Cogn Sci. 11:229–235.
Laird AR, Eickhoff SB, Fox PM, Uecker AM, Ray KL, Saenz JJ Jr, McKay DR, Bzdok D, Laird RW, Robinson JL et al. 2011. The BrainMap strategy for standardization, sharing, and meta-analysis of neuroimaging data. BMC Res Notes. 4:349.
Laird AR, Eickhoff SB, Kurth F, Fox PM, Uecker AM, Turner JA, Robinson JL, Lancaster JL, Fox PT. 2009. ALE meta-analysis workflows via the BrainMap database: progress towards a probabilistic functional brain atlas. Front Neuroinformatics. 3:23.
Liston C, Matalon S, Hare TA, Davidson MC, Casey BJ. 2006. Anterior cingulate and posterior parietal cortices are sensitive to dissociable forms of conflict in a task-switching paradigm. Neuron. 50:643–653.
Lowe MJ, Dzemidzic M, Lurito JT, Mathews VP, Phillips MD. 2000. Correlations in low-frequency BOLD fluctuations reflect cortico-cortical connections. Neuroimage. 12:582–587.
Lu MT, Preston JB, Strick PL. 1994. Interconnections between the prefrontal cortex and the premotor areas in the frontal lobe. J Comp Neurol. 341:375–392.
MacDonald AW, Cohen JD, Stenger VA, Carter CS. 2000. Dissociating the role of the dorsolateral prefrontal and anterior cingulate cortex in cognitive control. Science. 288:1835–1838.
Mansouri FA, Tanaka K, Buckley MJ. 2009. Conflict-induced behavioural adjustment: a clue to the executive functions of the prefrontal cortex. Nat Rev Neurosci. 10:141–152.
Mars RB, Sallet J, Schüffelgen U, Saad J, Toni I, Rushworth FS. 2011. Connectivity-based subdivisions of the human right "temporoparietal junction area": evidence for different areas participating in different cortical networks. Cereb Cortex. 22:1894–1903.
Menon V, Adleman NE, White CD, Glover GH, Reiss AL. 2001. Error-related brain activation during a Go/NoGo response inhibition task. Hum Brain Mapp. 12:131 –143.
Menon V, Uddin LQ. 2010. Saliency, switching, attention and control: a network model of insula function. Brain Struct Funct. 214(5–6):655–667.
Miller EK, Cohen JD. 2001. An integrative theory of prefrontal cortex function. Annu Rev Neurosci. 24:167–202.
Nebel K, Wiese H, Stude P, de Greiff A, Diener HS, Keidel M. 2005. On the neural basis of focused and divided attention. Brain Res Cogn Brain Res. 25:760–776.
Nee DE, Wager TD, Jonides J. 2007. Interference resolution: insights from a meta-analysis of neuroimaging tasks. Cogn Affect Behav Neurosci. 7:1–17.
Passingham D, Sakai K. 2004. The prefrontal cortex and working memory: physiology and brain imaging. Curr Opin Neurobiol. 14:163–168.
Petrides M, Pandya DN. 1999. Dorsolateral prefrontal cortex: comparative cytoarchitectonic analysis in the human and the macaque brain and corticocortical connection patterns. Eur J Neurosci. 11:1011–1036.
Petrides M, Pandya DN. 1984. Projections to the frontal cortex from the posterior parietal region in the rhesus monkey. J Comp Neurol. 228:105–116.
Peyron R, Laurent B, Garcia-Larrea L. 2000. Functional imaging of brain responses to pain. A review and meta-analysis. Neurophysiol Clin. 30:263 –288.
Poldrack AR. 2006. Can cognitive processes be inferred from neuroimaging data? Trends Cogn Sci. 10(2):59–63.
Poldrack AR. 2011. Inferring mental states from neuroimaging data: from reverse inference to large-scale decoding. Neuron. 72 (5):692–697.
Ridderinkhof KR, Ullsperger M, Crone EA, Nieuwenhuis S. 2004. The role of the medial frontal cortex in cognitive control. Science. 306 (5695):443–447.
Robinson JL, Laird AR, Glahn DC, Lovallo WR, Fox PT. 2010. Metaanalytic connectivity modeling: delineating the functional connectivity of the human amygdala. Hum Brain Mapp. 31:173–184.
Rottschy C, Eickhoff SB, Schleicher A, Mohlberg H, Kujovic M, Zilles K, Amunts K. 2007. Ventral visual cortex in humans: cytoarchitectonic mapping of two extrastriate areas. Hum Brain Mapp. 28:1045–1059.

Scheperjans F, Eickhoff SB, Homke L, Mohlberg H, Hermann K, Amunts K, Zilles K. 2008. Probabilistic maps, morphometry, and variability of cytoarchitectonic areas in the human superior parietal cortex. Cereb Cortex. 18:2141–2157.
Scheperjans F, Hermann K, Eickhoff SB, Amunts K, Schleicher A, Zilles K. 2008. Observer-independent cytoarchitectonic mapping of the human superior parietal cortex. Cereb Cortex. 18:846–867.
Schmahmann JD, Pandya DN. 1997. Anatomic organization of the basilar pontine projections from prefrontal cortices in rhesus monkey. J Neurosci. 17:438–458.
Shallice T. 2004. The fractionation of supervisory control. In: Gazzaniga MS. The Cognitive Neuroscience, 3rd ed. Cambridge, MA: MIT Press. p. 943–956.
Sohn MH, Albert MV, Jung K, Carter CS, Anderson JR. 2007. Anticipation of conflict monitoring in the anterior cingulate cortex and the prefrontal cortex. Proc Natl Acad Sci USA. 104:10330–10334.
Taren AA, Venkatraman V, Huettel SA. 2011. A parallel functional topography between medial and lateral prefrontal cortex: evidence and implications for cognitive control. J Neurosci. 31:5026–5031.
Thompson KG, Bichot NP. 2005. A visual salience map in the primate frontal eye field. Progr Brain Res. 147:251–262.
Timm NH. 2002. Applied Multivariate Analysis. New York: Springer.
Tsujimoto A, Genovesio A, Wise SP. 2011. Comparison of strategy signals in the dorsolateral and orbital prefrontal cortex. J Neurosci. 31(12):4583–4592.
Turkeltaub PE, Eickhoff SB, Laird AR, Fox M, Wiener M, Fox P. 2012. Minimizing within-experiment and within-group effects in Activation Likelihood Estimation meta-analyses. Hum Brain Mapp. 33:1–13.
Turner JA, Laird AR. 2012. The cognitive paradigm ontology: design and application. Neuroinformatics. 10(1):57–66.
van den Heuvel MP, Hulshoff Pol HE. 2010. Exploring the brain network: a review on resting-state fMRI functional connectivity. Eur Neuropsychopharmacol. 20:519–534.
van den Heuvel MP, Mandl RC, Kahn RS, Hulshoff Pol HE. 2009. Functionally linked resting-state networks reflect the underlying structural connectivity architecture of the human brain. Hum Brain Mapp. 30:3127–3141.
Vogt S, Buccino G, Wohlschlager AM, Canessa N, Shah NJ, Zilles K, Eickhoff SB, Freund HJ, Rizzolatti G, Fink GR. 2007. Prefrontal involvement in imitation learning of hand actions: effects of practice and expertise. Neuroimage. 37:1371–1383.
Walker AE. 1940. A cytoarchitectual study of the prefrontal area of the macaque monkey. J Comp Neurol. 73:59–86.
Womelsdorf T, Fries P. 2007. The role of neuronal synchronization in selective attention. Curr Opin Neurobiol. 17:154–160.
Wood JN, Grafman J. 2003. Human prefrontal cortex: processing and representational perspectives. Nat Rev Neurosci. 4:139–147.
Yamaguchi S, Zheng D, Oka T, Bokura H, 2008. The key locus of common response inhibition network for no-go and stop signals. J Cogn Neurosci. 20:1434–1442.
Yarkoni T, Poldrack RA, Nichols TE, Van Essen DC, Wager TD. 2011. Large-scale automated synthesis of human functional neuroimaging data. Nat Methods. 8:665–670.